IEEE Access
Multidisciplinary : Rapid Review : Open Access Journal

Received August 26, 2019, accepted September 6, 2019, date of publication September 13, 2019, date of current version September 26, 2019.

Digital Object Identifier 10.1109/ACCESS.2019.2941386

A Fully Distributed Coordination Method for Fast Decoupled Multi-Region State Estimation

ZHENGWEI REN[1], YING CHEN[1], (Member, IEEE), SHAOWEI HUANG[1], (Member, IEEE), MIGUEL HELENO[2], AND YUE XIA[1], (Member, IEEE)

[1]Department of Electrical Engineering, Tsinghua University, Beijing 100084, China
[2]Lawrence Berkeley National Laboratory, Energy Storage and Distributed Resources Division, Berkeley, CA 94720, USA

Corresponding author: Shaowei Huang (huangsw@mail.tsinghua.edu.cn)

This work was supported in part by the National Natural Science Foundation of China under Grant 51477081 and Grant 51877115.

ABSTRACT Distributed state estimation (DSE) is effective for the analysis of multi-region state estimation problems, avoiding integrating complicated data sets and models. In this work, the peer-to-peer decomposition of the Karush-Kuhn-Tucker (KKT) condition is applied to formulate the fully distributed fast decoupled state estimation (FD2SE) algorithm. Then, a fixed-matrix form data-exchanging interface incorporating the fast decoupled algorithm is designed, reducing the communication costs and allowing it to be used for various system operating conditions. Further, a convergence detecting method for dispatch centers is proposed in order to infer, locally and asynchronously, about the global convergence. Case studies carried out on IEEE systems and a real power grid of China verify the accuracy and efficiency of the FD2SE algorithm.

INDEX TERMS Fully distributed state estimation, data-exchanging interface, asynchronous convergence detecting.

I. INTRODUCTION

A. MOTIVATION

Accurate state estimation (SE) of interconnected power systems is critical for assessing system security and optimizing performances. [1], [2]. This becomes particularly challenging for continental-scale power systems that rely on the coordination of multiple dispatch centers, while each one of the dispatch centers controls a large-scale region. The distributed state estimation (DSE) is mostly implemented in these continental-scale systems [3], since centrally SE approaches require impractical amounts of data, assembling of complicated models and heavy computational burden.

Among DSE, hierarchical approaches (HDSE) are based on centralized iterative coordination, originating significant communication bottlenecks, especially in high dimensional systems. Thus, continental-scale SE has to rely on fully distributed approaches. On the other hand, each region of a continental power system corresponds to a large-scale transmission network, which requires a SE methodology with the low computational burden and high efficiency in handling real-time measurements. Hence, in practical energy management systems (EMSs), fast decoupled state estimation (FDSE) [4]–[6] has become the widely adopted algorithm for interconnected large-scale power systems.

In short, realistic approaches to SE in continental-scale systems tend to be fully distributed and depend on FDSE in each regional dispatch center. However, coordinating these multiple large-scale dispatch centers is a major challenge. In fact, due to the dimensions of the system, convergence rate is crucial to ensure the practicality of the SE solution. To address this problem, this paper proposes a new method for coordinating multiple large-scale dispatch centers in continental-scale power systems. The proposed methodology takes advantage of the proprieties of the regional FDSE to improve the efficiency of multi-region coordination. This improvement is achieved by decentralizing the coordination process itself, allowing a natural articulation with the regional FDSE and accelerating the SE process. This fully distributed fast decoupled state estimation (FD2SE) realizes the decentralized coordination of FDSE among regional power grids, and enables the online application in large-scale interconnected power systems.

B. RELATED WORKS

Different methods to achieve the coordinated solution of the multi-region SE can be found in the literature. These methods

The associate editor coordinating the review of this manuscript and approving it for publication was Yinliang Xu.

can be classified into HDSE approaches and fully distributed SE approaches. In the HDSE approaches, the Karush-Kuhn-Tucker (KKT) condition decomposition [7] is widely adopted, which possesses high convergence rate, but requires a centralized communication, thus originating bottlenecks. Fully distributed SE approaches can be found in alternating direction method of multipliers (ADMM) [8], [9], matrix splitting technique [10], [11], gossip-based algorithm [12], [13], and distributed subgradient algorithm [14]. In ADMM, the distributed framework for solving multi-region SE can be realized by introducing an auxiliary variable. The ADMM-based SE can also model influences caused by cyber-attacks [8], [15] and communication errors [16], by introducing outlier variables or attack variables, which makes the multi-region SE more robust. In the matrix splitting technique, the Jacobian matrix of the Newton iteration is divided into two sub-matrices, which allows the Gauss-Newton to be computed iteratively in a fully distributed manner. Gossip-based algorithms implement the fully distributed decomposition using an aggregate state to evolve the state vectors, imposing no limitations on the communication systems [12]. The distributed subgradient algorithm proposed in [14] is able to solve both topology identification and multi-region SE problems. It achieves the fully distributed coordination and possesses good flexibility and reliability. In practice, these algorithms may require great modification of data and models in the EMS of continental-scale grids. Therefore, new coordination methods should be put forward with less dependency on communication, and more adaptability to reuse data and matrices from local SE results.

Amount of data exchange required is another critical aspect of DSE performance. Therefore, innovative data interface designs have been proposed to reduce the communication burden. For example, the data interface can be designed in matrix form and expressed as a sensitivity function, incorporating both gradient vectors and gain matrices [7] or Lagrange multipliers [17]. Inherited from the classic weighted least square (WLS) SE method [18], these matrix-form interfaces show good performance in terms of convergence rate, but may demand significant data communication efforts. An alternative design of data interface is formulated by transmitting the states of boundary buses. In [10], [11] where matrix splitting technique is applied, boundary states are communicated among neighboring grids. Moreover, in [19], the boundary states are computed by regional estimators and then sent to the central coordinator, which views the boundary states as pseudo-measurements and uses synchronized phasor measurements to process the local SE results. In [20], an efficient data interface for solving DSE is designed, considering the measurements weight update [21] during the boundary states exchange. Compared with the matrix-form data interface, this approach requires less amount of communication burden. This paper aims to develop a data interface based on the FDSE algorithm, obtaining its fast convergence rate, minor amount of data communication and good estimation quality [22].

Furthermore, solving multi-region SE requires dispatch centers to judge the global convergence accurately and stop the computation promptly. In HDSE approaches the computation in regional grids is synchronous and the global convergence can be judged only by the coordinator [7]. However, in fully distributed SE, each local dispatch center is a decision agent whose knowledge is limited to its own governing region. Judging the global convergence in these conditions depends on the coordination method. In ADMM [9], a primal and dual residual vector is defined for each boundary and the convergence is judged through this residual vector. In matrix splitting method [11], a maximum iteration number is given to truncate the distributed computation. In the gossip-based algorithm [13], an observability restoration process is conducted to guarantee that all regions are global observable and local states are used to check the overall convergence. Above coordination methods in fully distributed SE achieve the local detection of global convergence, but the computation in regional dispatch centers is still carried out synchronously. Therefore, to further improve performance of the multi-region SE, innovative algorithms should encompass the asynchronous stopping criteria for regional grids.

C. CONTRIBUTIONS

In this work, an FD2SE algorithm is proposed to solve the SE of continental-scale interconnected power systems. The main contributions are as follows:

1) Peer-to-Peer coordination of multi-region SE is proposed to apply the fully distributed approach, which eliminates interactions among states of different boundary buses. The KKT condition of the global SE problem is decomposed according to territories of regional transmission grids.

2) Data-exchanging interface for peer-to-peer coordination is designed based on the FDSE method, and presented in the form of fixed Jacobian matrices. Such interface shows good performance in fast convergence rate, low data exchange burden, and keeps its stability under various load levels of regional power grids.

3) Local detection of the global convergence is enabled in the FD2SE, while the asynchronous stopping criteria is put forward for regional dispatch centers. A scale factor relating to grid parameters is specified, which provides a feasible condition for regional grids to judge the convergence and stop computation promptly.

Moreover, the FD2SE algorithm is able to deal with both SCADA and PMU measurements. It is also tested through IEEE benchmark systems and a real power grid of southwest China. The high computational efficiency and good convergence rate of the proposed FD2SE algorithm have been verified under different connection patterns and multiple load levels.

D. PAPER ORGANIZATION

The paper is organized as follows. Section II gives the models of multi-region SE and illustrates the workflow of the fully distributed SE. Section III develops the peer-to-peer

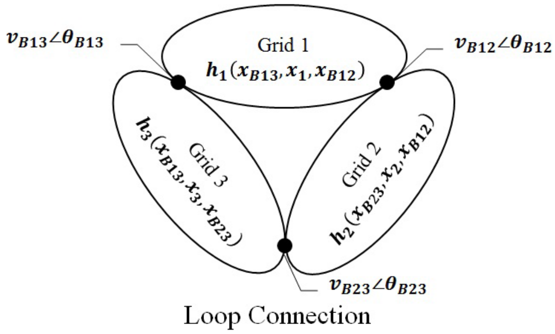

FIGURE 1. Connecting pattern of multi-region power grids.

coordination of multi-region SE. In Section IV, a data-exchanging interface is designed by integrating the fast decoupled algorithm. In Section V, the FD2SE algorithm is presented, and a method is proposed to detect the global convergence locally and asynchronously. Section VI gives the test results on three different systems, and the conclusion is given in Section VII.

II. PROBLEM DESCRIPTION

A. SE OF INTERCONNECTED POWER SYSTEMS

Generally, the basic model of the WLS-based SE is formulated as below

$$min : \boldsymbol{J}(\boldsymbol{x}) = [z - \boldsymbol{h}(\boldsymbol{x})]^T \boldsymbol{G}[z - \boldsymbol{h}(\boldsymbol{x})], \tag{1}$$

where state vector $\boldsymbol{x}$ includes both bus voltage amplitudes and phase angles. z represents a vector of measurements, which usually consists of bus voltage amplitudes, phase angles (if PMU measurements are used), bus injected powers and line powers. Measurement function $\boldsymbol{h}(\boldsymbol{x})$ is a nonlinear mapping from $\boldsymbol{x}$ to z, according to the AC power flow model. The superscript T means to transpose a vector or matrix. $\boldsymbol{G}$ is a weighting matrix, which is given according to the quality of measurements. If interconnected power systems are studied, a multi-region SE formulation needs to be established for estimating both inner-region states and states of boundary buses.

Without loss of generality, we take the interconnected power system shown in Fig. 1 as an example of the following theoretical derivation.

It can be seen from Fig. 1 that three regional power grids are connected with each other by the boundary buses. The overall measurement vector z can be represented as $z = [z_1, z_2, z_3]^T$. Similarly, the measurement function is also reformed as $\boldsymbol{h} = [\boldsymbol{h}_1, \boldsymbol{h}_2, \boldsymbol{h}_3]^T$. The state vector contains internal bus states and boundary states as $\boldsymbol{x} = [\boldsymbol{x}_1, \boldsymbol{x}_2, \boldsymbol{x}_3, \boldsymbol{x}_{B12}, \boldsymbol{x}_{B23}, \boldsymbol{x}_{B13},]^T$. $\boldsymbol{x}_1$, $\boldsymbol{x}_2$ and $\boldsymbol{x}_3$ are the internal bus states corresponding to three regional power grids respectively, while $\boldsymbol{x}_{B12} = \boldsymbol{v}_{B12}\angle\theta_{B12}, \boldsymbol{x}_{B23} = \boldsymbol{v}_{B23}\angle\theta_{B23}$, and $\boldsymbol{x}_{B13} = \boldsymbol{v}_{B13}\angle\theta_{B13}$ are states of boundary buses. $\boldsymbol{v}_{B12}, \boldsymbol{v}_{B23}, \boldsymbol{v}_{B13}$ are voltage amplitudes of boundary buses, and $\theta_{B12}, \theta_{B23}, \theta_{B13}$ are phase angles of boundary buses.

Then, (1) can be rewritten as below,

$$\begin{aligned} min: &\boldsymbol{J}(\boldsymbol{x}_1, \boldsymbol{x}_2, \boldsymbol{x}_3, \boldsymbol{x}_{B12}, \boldsymbol{x}_{B23}, \boldsymbol{x}_{B13}) \\ &= \begin{bmatrix} z_1 - \boldsymbol{h}_1 \\ z_2 - \boldsymbol{h}_2 \\ z_3 - \boldsymbol{h}_3 \end{bmatrix}^T \begin{bmatrix} \boldsymbol{G}_1 & & \\ & \boldsymbol{G}_2 & \\ & & \boldsymbol{G}_3 \end{bmatrix} \begin{bmatrix} z_1 - \boldsymbol{h}_1 \\ z_2 - \boldsymbol{h}_2 \\ z_3 - \boldsymbol{h}_3 \end{bmatrix} \\ &= \boldsymbol{J}_1(\boldsymbol{x}_{B13}, \boldsymbol{x}_1, \boldsymbol{x}_{B12}) + \boldsymbol{J}_2(\boldsymbol{x}_{B12}, \boldsymbol{x}_2, \boldsymbol{x}_{B23}) \\ &\quad + \boldsymbol{J}_3(\boldsymbol{x}_{B23}, \boldsymbol{x}_3, \boldsymbol{x}_{B13}) \end{aligned} \tag{2}$$

where $\boldsymbol{h}_1, \boldsymbol{h}_2$, and $\boldsymbol{h}_3$ is short for $\boldsymbol{h}_1(\boldsymbol{x}_{B13}, \boldsymbol{x}_1, \boldsymbol{x}_{B12})$, $\boldsymbol{h}_2(\boldsymbol{x}_{B12}, \boldsymbol{x}_2, \boldsymbol{x}_{B23})$ and $\boldsymbol{h}_3(\boldsymbol{x}_{B23}, \boldsymbol{x}_3, \boldsymbol{x}_{B13})$, respectively. $\boldsymbol{J}_i = [z_i - \boldsymbol{h}_i]^T \boldsymbol{G}_i [z_i - \boldsymbol{h}_i], i = 1, 2, 3$ represents the local SE of regional power grids. It can be seen that these regional SE equations are coupled through their boundary states.

B. SOLVING MULTI-REGION SE IN A FULLY DISTRIBUTED WAY

Normally, each regional power grid is governed by a local dispatch center, where an EMS is equipped for online monitoring and analyzing applications. It is assumed that there is a SE module installed in such an EMS platform. Moreover, communications between dispatch centers are also assumed to be enabled. However, intra-site communications are performed on the Wide Area Network (WAN), where high latencies may be encountered.

Through data exchange, a dispatch center can obtain supplementary information, which could make its local SE converge to a more accurate result. That is, by coordinating local SE solutions, the global converged SE results of the whole interconnected power systems can be achieved without assembling all network parameters and measurements from regional power grids. Moreover, it is further assumed in this work that there is no centralized coordinator controlling such distributed SE computations. On the contrary, in each dispatch center, a local coordinator is developed, which determines boundary information driving the local SE solution. It has two functions, such as 1) exchanging boundary information with neighboring local dispatch centers; 2) updating states of boundary buses required for the local SE solution. All local coordinators work together and update boundary information iteratively in a fully distributed way, in order to drive local SE solutions to converge global SE results.

Generally, to ensure the security of coordinated operations, there are communication channels among dispatch centers of adjacent regions, which are in the private communication network serving power grids. Through such communication channels, the boundary information is exchanged to facilitate the distributed state estimation. The non-adjacent regions can exchange data through other dispatch centers indirectly, which may require more data-exchange cost and longer latency, resulting in communication errors. In this paper, we consider the minimal communication requirement, where only communication among neighboring regions is needed. By reducing the complexity of the communication scheme, the FD2SE could be more efficient, reliable and easier to be implemented.

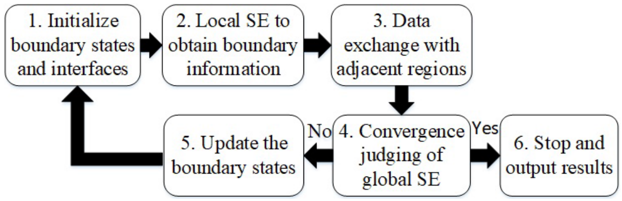

FIGURE 2. **Workflow of fully distributed SE.**

Fig. 2 presents the ideal workflow of the fully distributed SE of interconnected power systems.

It can be seen that in the fully distributed SE, each dispatch center initiates its local SE to obtain the boundary information. Then, the dispatch center exchanges boundary information only with adjacent regions, and performs the convergence judging for the global SE. If the global SE is not converged, boundary states are updated and local SE is carried out again. Otherwise, stop the fully distributed SE and output the results. There are three challenges in implementing the above fully distributed SE, which are handled in the following sections.

1) To enable fully distributed SE, a peer-to-peer coordination model needs to be formulated carefully. Then, a conflict must be solved when developing such a model. That is, to ensure global convergence of the distributed SE, influences of boundary information variations on all regional SE solutions should be considered during iterative coordination. Meanwhile, the peer-to-peer coordination requires that only boundary information from neighboring regional power grids can be used in the local SE solution.

2) As mentioned before, the FDSE is widely used in local EMS platforms due to its computational efficiency and numerical stability. Thus, it is reasonable to implement fully distributed SE with suitable boundary interfaces to FDSE functions. Moreover, to avoid communication overheads, such an interface should adopt a fixed coefficient matrix which can be formed before the distributed coordination.

3) Without a centralized coordinator, detecting the global convergence of the distributed SE tends to be a difficult problem. One possible solution is to stop local coordination automatically and asynchronously. That is, let each local coordinator stop working once states of boundary buses change little in successive iterations. Then, to guarantee accurate results of the global SE, sufficient conditions for these asynchronous stopping criteria should be given and checked before conducting the proposed fully distributed SE.

III. PEER-TO-PEER COORDINATION OF MULTI-REGION SE

A. DECOMPOSITION OF GLOBAL KKT CONDITION

The solution of (2) should satisfy the following equation, which is also named as the KKT condition,

$$\partial \boldsymbol{J}(\boldsymbol{x})/\partial \boldsymbol{x} = -\boldsymbol{H}^T \boldsymbol{G}[z - \boldsymbol{h}(\boldsymbol{x})] = \boldsymbol{0} \tag{3}$$

where $\boldsymbol{H} = \partial \boldsymbol{h}(\boldsymbol{x})/\partial \boldsymbol{x}$ is the Jacobian matrix.

Apply the Taylor expansion to $\boldsymbol{h}(\boldsymbol{x})$ in (3), and neglect the higher order terms, then the correction formula for solving (2) can be derived as below.

$$\left(\boldsymbol{H}^T \boldsymbol{G}\boldsymbol{H}\right)\Delta \boldsymbol{x} = \boldsymbol{H}^T \boldsymbol{G}(z - \boldsymbol{h}(\boldsymbol{x})) \tag{4}$$

That is, $\boldsymbol{x}$ is iteratively updated according to (4), until the infinite norm of $\Delta \boldsymbol{x}$ is smaller than a given tolerance.

For the interconnected power systems in Fig. 1, the KKT condition of global SE (3) can be decomposed according to territories of regional power grids as follows,

$$\begin{cases} \dfrac{\partial \boldsymbol{J}_1(\boldsymbol{x}_{B13}, \boldsymbol{x}_1, \boldsymbol{x}_{B12})}{\boldsymbol{x}_1} = \boldsymbol{0} & \text{(5a)} \\ \dfrac{\partial \boldsymbol{J}_2(\boldsymbol{x}_{B12}, \boldsymbol{x}_2, \boldsymbol{x}_{B23})}{\boldsymbol{x}_2} = \boldsymbol{0} & \text{(5b)} \\ \dfrac{\partial \boldsymbol{J}_3(\boldsymbol{x}_{B23}, \boldsymbol{x}_3, \boldsymbol{x}_{B13})}{\boldsymbol{x}_3} = \boldsymbol{0} & \text{(5c)} \\ \dfrac{\partial \boldsymbol{J}_1(\boldsymbol{x}_{B13}, \boldsymbol{x}_1, \boldsymbol{x}_{B12})}{\boldsymbol{x}_{B12}} + \dfrac{\partial \boldsymbol{J}_2(\boldsymbol{x}_{B12}, \boldsymbol{x}_2, \boldsymbol{x}_{B23})}{\boldsymbol{x}_{B12}} = \boldsymbol{0} & \text{(5d)} \\ \dfrac{\partial \boldsymbol{J}_2(\boldsymbol{x}_{B12}, \boldsymbol{x}_2, \boldsymbol{x}_{B23})}{\boldsymbol{x}_{B23}} + \dfrac{\partial \boldsymbol{J}_3(\boldsymbol{x}_{B23}, \boldsymbol{x}_3, \boldsymbol{x}_{B13})}{\boldsymbol{x}_{B23}} = \boldsymbol{0} & \text{(5e)} \\ \dfrac{\partial \boldsymbol{J}_3(\boldsymbol{x}_{B23}, \boldsymbol{x}_3, \boldsymbol{x}_{B13})}{\boldsymbol{x}_{B13}} + \dfrac{\partial \boldsymbol{J}_1(\boldsymbol{x}_{B13}, \boldsymbol{x}_1, \boldsymbol{x}_{B12})}{\boldsymbol{x}_{B13}} = \boldsymbol{0} & \text{(5f)} \end{cases}$$

where (5a)-(5c) refer to the KKT condition of local SEs. (5d)-(5f) represent the coupled relations among local KKT condition. If all these 6 equations are satisfied, the global SE converges to a solution.

B. COORDINATING LOCAL SE WITH GIVEN BOUNDARY BUS STATES

It can be seen that if $\boldsymbol{x}_{B12}$ and $\boldsymbol{x}_{B13}$ are given, variables in (5a) are only internal bus states of region 1. That is, with given values of boundary bus states, a local SE can be solved to obtain internal bus states. Then, we can have implicit mappings as $\boldsymbol{x}_1 = \varphi_1(\boldsymbol{x}_{B12}, \boldsymbol{x}_{B13})$, $\boldsymbol{x}_2 = \varphi_2(\boldsymbol{x}_{B12}, \boldsymbol{x}_{B23})$ and $\boldsymbol{x}_3 = \varphi_3(\boldsymbol{x}_{B23}, \boldsymbol{x}_{B13})$. φ_1, φ_2, and φ_3 actually represent the local SEs constrained by boundary bus states.

Generally, the DSE can be carried out by two steps. **Step 1**: With fixed values of boundary bus states, local SEs are performed to estimate the internal bus states. **Step 2**: With estimated results of internal bus states, the boundary states are estimated through coordinating equations. These two steps are performed iteratively until the final solution is obtained. The convergence and optimality of the DSE are given by the following theorem [7].

Theorem 1: In the neighborhood of the optimal solution, if the Hessian matrix of the overall SE is positive definite, while φ_1, φ_2 and φ_3 are bounded and Frechet-differentiable. Then the DSE can converge to the same optimal state estimate as the centralized state estimation (CSE) does, and its convergence rate is the same as the Gauss-Newton algorithm.

The proof of the theorem is given in [7], which also elaborates that the preconditions in Theorem 1 can be easily satisfied by real power grids.

$$
\begin{cases}
\frac{\partial \boldsymbol{h}_1^T}{\partial \boldsymbol{x}_1}\boldsymbol{G}_1\frac{\partial \boldsymbol{h}_1}{\partial \boldsymbol{x}_1}\Delta \boldsymbol{x}_1+\frac{\partial \boldsymbol{h}_1^T}{\partial \boldsymbol{x}_1}\boldsymbol{G}_1\frac{\partial \boldsymbol{h}_1}{\partial \boldsymbol{x}_{B12}}\Delta \boldsymbol{x}_{B12}+\frac{\partial \boldsymbol{h}_1^T}{\partial \boldsymbol{x}_1}\boldsymbol{G}_1\frac{\partial \boldsymbol{h}_1}{\partial \boldsymbol{x}_{B13}}\Delta \boldsymbol{x}_{B13}=\frac{\partial \boldsymbol{h}_1^T}{\partial \boldsymbol{x}_1}\boldsymbol{G}_1\left(z_1-\boldsymbol{h}_1\right) & (7)\\
\frac{\partial \boldsymbol{h}_2^T}{\partial \boldsymbol{x}_2}\boldsymbol{G}_2\frac{\partial \boldsymbol{h}_2}{\partial \boldsymbol{x}_{B12}}\Delta \boldsymbol{x}_{B12}+\frac{\partial \boldsymbol{h}_2^T}{\partial \boldsymbol{x}_2}\boldsymbol{G}_2\frac{\partial \boldsymbol{h}_2}{\partial \boldsymbol{x}_2}\Delta \boldsymbol{x}_2+\frac{\partial \boldsymbol{h}_2^T}{\partial \boldsymbol{x}_2}\boldsymbol{G}_2\frac{\partial \boldsymbol{h}_2}{\partial \boldsymbol{x}_{B23}}\Delta \boldsymbol{x}_{B23}=\frac{\partial \boldsymbol{h}_2^T}{\partial \boldsymbol{x}_2}\boldsymbol{G}_2\left(z_2-\boldsymbol{h}_2\right) & (8)\\
\frac{\partial \boldsymbol{h}_1^T}{\partial \boldsymbol{x}_{B12}}\boldsymbol{G}_1\frac{\partial \boldsymbol{h}_1}{\partial \boldsymbol{x}_1}\Delta \boldsymbol{x}_1+\left[\frac{\partial \boldsymbol{h}_1^T}{\partial \boldsymbol{x}_{B12}}\boldsymbol{G}_1\frac{\partial \boldsymbol{h}_1}{\partial \boldsymbol{x}_{B12}}+\frac{\partial \boldsymbol{h}_2^T}{\partial \boldsymbol{x}_{B12}}\boldsymbol{G}_2\frac{\partial \boldsymbol{h}_2}{\partial \boldsymbol{x}_{B12}}\right]\Delta \boldsymbol{x}_{B12}+\frac{\partial \boldsymbol{h}_2^T}{\partial \boldsymbol{x}_{B12}}\boldsymbol{G}_2\frac{\partial \boldsymbol{h}_2}{\partial \boldsymbol{x}_2}\Delta \boldsymbol{x}_2+\frac{\partial \boldsymbol{h}_2^T}{\partial \boldsymbol{x}_{B12}}\boldsymbol{G}_2\frac{\partial \boldsymbol{h}_2}{\partial \boldsymbol{x}_{B23}}\Delta \boldsymbol{x}_{B23} & \\
\quad +\frac{\partial \boldsymbol{h}_1^T}{\partial \boldsymbol{x}_{B12}}\boldsymbol{G}_1\frac{\partial \boldsymbol{h}_1}{\partial \boldsymbol{x}_{B13}}\Delta \boldsymbol{x}_{B13}=\frac{\partial \boldsymbol{h}_1^T}{\partial \boldsymbol{x}_{B12}}\boldsymbol{G}_1\left(z_1-\boldsymbol{h}_1\right)+\frac{\partial \boldsymbol{h}_2^T}{\partial \boldsymbol{x}_{B12}}\boldsymbol{G}_2\left(z_2-\boldsymbol{h}_2\right) & (9)
\end{cases}
$$

C. PEER-TO-PEER COORDINATING EQUATION OF BOUNDARY BUS STATES

Considering 3 regional grids, the Jacobian matrix $\boldsymbol{H}$ can be rewritten as below,

$$
\boldsymbol{H}=\begin{bmatrix}
\frac{\partial \boldsymbol{h}_1}{\partial \boldsymbol{x}_1} & 0 & 0 & \frac{\partial \boldsymbol{h}_1}{\partial \boldsymbol{x}_{B12}} & 0 & \frac{\partial \boldsymbol{h}_1}{\partial \boldsymbol{x}_{B13}}\\
0 & \frac{\partial \boldsymbol{h}_2}{\partial \boldsymbol{x}_2} & 0 & \frac{\partial \boldsymbol{h}_2}{\partial \boldsymbol{x}_{B12}} & \frac{\partial \boldsymbol{h}_2}{\partial \boldsymbol{x}_{B23}} & 0\\
0 & 0 & \frac{\partial \boldsymbol{h}_3}{\partial \boldsymbol{x}_3} & 0 & \frac{\partial \boldsymbol{h}_3}{\partial \boldsymbol{x}_{B23}} & \frac{\partial \boldsymbol{h}_3}{\partial \boldsymbol{x}_{B13}}
\end{bmatrix} \tag{6}
$$

Substitute (6) into (4), then the correction formula for the multi-region SE is obtained for coordinating local SEs. Here, only correction formulas of states in region 1 and region 2 as well as their boundaries are given. That is, (7), (8) and (9), as shown at the top of this page, are correction formulas corresponding to (5a), (5b) and (5d) respectively. Especially, (9) is denoted as the coordinating equation for boundary B12.

Obviously, $\boldsymbol{x}_{B23}$ and $\boldsymbol{x}_{B13}$ are still included in (9), which represent remote-coupling relations of local SEs. Thus, to enable purely peer-to-peer coordination, such remote-coupling should be removed carefully. A corresponding solution is to drop items in (9) related to $\boldsymbol{x}_{B23}$ and $\boldsymbol{x}_{B13}$. Then, only states and coefficients about region 1 and region 2 remain. It can be proven that when the following condition is satisfied, such a solution would be feasible for formulating peer-to-peer coordinating equations of DSE applications.

Condition A: Buses on every two different boundaries are not directly connected.

It should be noted that in a large scale power system, a regional grid may stretch across wide areas. Boundaries of different neighboring grids are normally not connected with each other directly. Under such a circumstance, the condition A can be satisfied. Take the multi-region power grids given by Fig. 1 as an example. Condition A means that the boundary buses of B12 are not directly connected to boundary buses of B23 or B13. Besides, for some small power systems, like those tested in the case study section, although the physical distances among different boundaries may not be very large, the electrical distances among boundaries may be large enough for ignoring cross-influences of their state variations. In fact, when the condition A is met, the following equation would be satisfied, which makes (9) only related to states of B12 and internal bus states of region 1 and region 2,

$$
\begin{cases}
\frac{\partial \boldsymbol{h}_1^T}{\partial \boldsymbol{x}_{B12}}\boldsymbol{G}_1\frac{\partial \boldsymbol{h}_1}{\partial \boldsymbol{x}_{B13}}=\boldsymbol{0} & (10a)\\
\frac{\partial \boldsymbol{h}_2^T}{\partial \boldsymbol{x}_{B12}}\boldsymbol{G}_2\frac{\partial \boldsymbol{h}_2}{\partial \boldsymbol{x}_{B23}}=\boldsymbol{0} & (10b)
\end{cases}
$$

To prove (10), let all available measurements be classified as internal and boundary ones, such as $\boldsymbol{h}_{1,in}$, $\boldsymbol{h}_{1,B12}$, and $\boldsymbol{h}_{1,B13}$. The $\boldsymbol{h}_{1,in}$ is only related to internal bus states, which can be denoted as $\boldsymbol{h}_{1,in}(\boldsymbol{x}_1)$. As for $\boldsymbol{h}_{1,B12}$ and $\boldsymbol{h}_{1,B13}$, thanks to condition A, boundary measurements are only related to states of nearby buses. Thus, they can be denoted as $\boldsymbol{h}_{1,B12}(\boldsymbol{x}_1,\boldsymbol{x}_{B12})$ and $\boldsymbol{h}_{1,B13}(\boldsymbol{x}_1,\boldsymbol{x}_{B13})$. Then, we have

$$
\boldsymbol{h}_1(\boldsymbol{x}_{B13},\boldsymbol{x}_1,\boldsymbol{x}_{B12})=\begin{bmatrix}\boldsymbol{h}_{1,B13}(\boldsymbol{x}_1,\boldsymbol{x}_{B13})\\ \boldsymbol{h}_{1,in}(\boldsymbol{x}_1)\\ \boldsymbol{h}_{1,B12}(\boldsymbol{x}_1,\boldsymbol{x}_{B12})\end{bmatrix}. \tag{11}
$$

Thus, the coefficient of $\Delta \boldsymbol{x}_{B13}$ in (9) can be expressed as

$$
\frac{\partial \boldsymbol{h}_1}{\partial \boldsymbol{x}_{B12}}^T\boldsymbol{G}_1\frac{\partial \boldsymbol{h}_1}{\partial \boldsymbol{x}_{B13}}=\begin{bmatrix}0\\0\\ \frac{\partial \boldsymbol{h}_{1,B12}}{\boldsymbol{x}_{B12}}\end{bmatrix}^T\boldsymbol{G}_1\begin{bmatrix}\frac{\partial \boldsymbol{h}_{1,B13}}{\boldsymbol{x}_{B13}}\\0\\0\end{bmatrix}=0. \tag{12}
$$

Similar derivations can be made for proving (10b). Finally, substitute (10) into (9) and eliminate the last two items on the left side of (9), the peer-to-peer coordinating equation can be obtained for local SEs of region 1 and region 2.

Actually, the peer-to-peer coordinating equation achieves the fully distributed coordination of the boundary state vectors. In (9), by eliminating items containing $\Delta \boldsymbol{x}_{B23}$ and $\Delta \boldsymbol{x}_{B13}$, adjustment of $\boldsymbol{x}_{B12}$ is only related to the local SEs of the adjacent regions. For boundaries B23 and B13, similar equations can be derived. Essentially, the fully distributed coordination is obtained from the KKT condition, by eliminating cross-boundary influences basing on condition A. Thus, the optimality and convergence given by Theorem 1 can also be applied to the fully distributed case.

$$\left(-\frac{\partial \boldsymbol{h}_1^T}{\partial \boldsymbol{x}_{B12}}\boldsymbol{G}_1\frac{\partial \boldsymbol{h}_1}{\partial \boldsymbol{x}_1}\left[\frac{\partial \boldsymbol{h}_1^T}{\partial \boldsymbol{x}_1}\boldsymbol{G}_1\frac{\partial \boldsymbol{h}_1}{\partial \boldsymbol{x}_1}\right]^{-1}\frac{\partial \boldsymbol{h}_1^T}{\partial \boldsymbol{x}_1}\boldsymbol{G}_1\frac{\partial \boldsymbol{h}_1}{\partial \boldsymbol{x}_{B12}}+\frac{\partial \boldsymbol{h}_1^T}{\partial \boldsymbol{x}_{B12}}\boldsymbol{G}_1\frac{\partial \boldsymbol{h}_1}{\partial \boldsymbol{x}_{B12}}+\frac{\partial \boldsymbol{h}_2^T}{\partial \boldsymbol{x}_{B12}}\boldsymbol{G}_2\frac{\partial \boldsymbol{h}_2}{\partial \boldsymbol{x}_{B12}}\right.$$
$$\left.-\frac{\partial \boldsymbol{h}_2^T}{\partial \boldsymbol{x}_{B12}}\boldsymbol{G}_2\frac{\partial \boldsymbol{h}_2}{\partial \boldsymbol{x}_2}\left[\frac{\partial \boldsymbol{h}_2}{\partial \boldsymbol{x}_2}^T\boldsymbol{G}_2\frac{\partial \boldsymbol{h}_2}{\partial \boldsymbol{x}_2}\right]^{-1}\frac{\partial \boldsymbol{h}_2}{\partial \boldsymbol{x}_2}^T\boldsymbol{G}_2\frac{\partial \boldsymbol{h}_2}{\partial \boldsymbol{x}_{B12}}\right)\Delta\boldsymbol{x}_{B12}=\frac{\partial \boldsymbol{h}_1}{\partial \boldsymbol{x}_{B12}}^T\boldsymbol{G}_1\left(\boldsymbol{z}_1-\boldsymbol{h}_1\right)+\frac{\partial \boldsymbol{h}_2}{\partial \boldsymbol{x}_{B12}}^T\boldsymbol{G}_2\left(\boldsymbol{z}_2-\boldsymbol{h}_2\right) \quad (15)$$

IV. DATA-EXCHANGING INTERFACE FOR PEER-TO-PEER COORDINATION

A. COORDINATING EQUATION FOR ADJUSTING BOUNDARY BUS STATES

It can be seen from (9), states of both boundary and internal buses are required to obtain proper adjustments of boundary bus states. To simplify the data-exchanging and reduce communication efforts, only boundary bus states should appear on the left-hand side of the coordinating equation.

It should be noted that the coordinating equation will be solved for adjusting boundary bus states only after neighboring local SEs converge. Thus, according to KKT condition given in (5a), items of the right side vector of (7) should all equal to zero, when solving (9). Moreover, during the peer-to-peer coordination of local SEs of region 1 and region 2, only the influence of $\Delta\boldsymbol{x}_{B12}$ on $\Delta\boldsymbol{x}_1$ is considered. Thus, we can set $\Delta\boldsymbol{x}_{B13}=0$ for further simplifying (7) as below,

$$\frac{\partial \boldsymbol{h}_1}{\partial \boldsymbol{x}_1}^T\boldsymbol{G}_1\frac{\partial \boldsymbol{h}_1}{\partial \boldsymbol{x}_1}\Delta\boldsymbol{x}_1=-\frac{\partial \boldsymbol{h}_1}{\partial \boldsymbol{x}_1}^T\boldsymbol{G}_1\frac{\partial \boldsymbol{h}_1}{\partial \boldsymbol{x}_{B12}}\Delta\boldsymbol{x}_{B12}. \quad (13)$$

Similar derivations can be carried out for (8),

$$\frac{\partial \boldsymbol{h}_2}{\partial \boldsymbol{x}_2}^T\boldsymbol{G}_2\frac{\partial \boldsymbol{h}_2}{\partial \boldsymbol{x}_2}\Delta\boldsymbol{x}_2=-\frac{\partial \boldsymbol{h}_2}{\partial \boldsymbol{x}_2}^T\boldsymbol{G}_2\frac{\partial \boldsymbol{h}_2}{\partial \boldsymbol{x}_{B12}}\Delta\boldsymbol{x}_{B12}. \quad (14)$$

Substitute (13) and (14) into (9). Then, we can have (15), as shown at the top of this page, where only $\Delta\boldsymbol{x}_{B12}$ is to solve. The right side of (15) contains two items, which are reallocations of local SE residuals on boundary bus B12. It can be seen that when local SEs converge, partial weighted residuals in both region 1 and region 2 should be allocated to boundary bus B12 according to the factors $\frac{\partial \boldsymbol{h}_1}{\partial \boldsymbol{x}_{B12}}$ and $\frac{\partial \boldsymbol{h}_2}{\partial \boldsymbol{x}_{B12}}$. If such residual reallocations are balanced on B12, which means the right side of (15) is a zero vector, there will be no needs for further adjusting boundary bus states $\Delta\boldsymbol{x}_{B12}$. Moreover, each item on the right side of (15), as shown in top of the page, can be obtained from the local SE result. Thus, they are denoted as regional residual allocation factors in the following contents.

B. DATA INTERFACE FOR INTEGRATING LOCAL FDSE

To integrate local FDSEs, the coordinating equation (15) should be adapted to the computation formulation of the conventional FDSE algorithm.

According to [22], partial derivatives of $\boldsymbol{h}_1$ and $\boldsymbol{h}_2$ can be approximated by certain fixed matrices born from the system admittance matrix. That is, we can have the following relations

$$\begin{cases}\frac{\partial \boldsymbol{h}_1}{\partial \boldsymbol{x}_1}\approx\boldsymbol{B}_1 & (16a)\\ \frac{\partial \boldsymbol{h}_2}{\partial \boldsymbol{x}_2}\approx\boldsymbol{B}_2 & (16b)\\ \frac{\partial \boldsymbol{h}_1}{\partial \boldsymbol{x}_{B12}}\approx\boldsymbol{B}_{B12}^1 & (16c)\\ \frac{\partial \boldsymbol{h}_2}{\partial \boldsymbol{x}_{B12}}\approx\boldsymbol{B}_{B12}^2 & (16d)\end{cases}$$

where $\boldsymbol{B}_1$, $\boldsymbol{B}_2$, $\boldsymbol{B}_{B12}^1$ and $\boldsymbol{B}_{B12}^2$ are approximations of original partial derivative matrices. Readers can refer to [22] for assumptions and derivations for dropping all variable factors in partial derivative matrices.

Then, (15) can be rewritten as (17),

$$\begin{aligned}&\left(\underbrace{\boldsymbol{B}_{B12}^1{}^T\boldsymbol{G}_1\left[-\boldsymbol{B}_1\left(\boldsymbol{B}_1^T\boldsymbol{G}_1\boldsymbol{B}_1\right)^{-1}\boldsymbol{B}_1^T\boldsymbol{G}_1\boldsymbol{B}_{B12}^1+\boldsymbol{B}_{B12}^1\right]}_{\boldsymbol{J}_{B12}^1}\right.\\&\left.\quad+\underbrace{\boldsymbol{B}_{B12}^2{}^T\boldsymbol{G}_2\left[-\boldsymbol{B}_2\left(\boldsymbol{B}_2^T\boldsymbol{G}_2\boldsymbol{B}_2\right)^{-1}\boldsymbol{B}_2^T\boldsymbol{G}_2\boldsymbol{B}_{B12}^2+\boldsymbol{B}_{B12}^2\right]}_{\boldsymbol{J}_{B12}^2}\right)\\&\quad\times\Delta\boldsymbol{x}_{B12}\\&=\boldsymbol{J}_{B12}\Delta\boldsymbol{x}_{B12}\\&=\underbrace{\boldsymbol{B}_{B12}^1{}^T\boldsymbol{G}_1\left(\boldsymbol{z}_1-\boldsymbol{h}_1\right)}_{\Delta\boldsymbol{F}_{B12}^1}+\underbrace{\boldsymbol{B}_{B12}^2{}^T\boldsymbol{G}_2\left(\boldsymbol{z}_2-\boldsymbol{h}_2\right)}_{\Delta\boldsymbol{F}_{B12}^2}\end{aligned} \quad (17)$$

where $\Delta\boldsymbol{F}_{B12}^1$ and $\Delta\boldsymbol{F}_{B12}^2$ are regional residual allocation factors. $\boldsymbol{J}_{B12}^1$ and $\boldsymbol{J}_{B12}^2$ are regional correction matrices provided by FDSE solutions of the region 1 and region 2 respectively. $\boldsymbol{J}_{B12}=\boldsymbol{J}_{B12}^1+\boldsymbol{J}_{B12}^2$ is the fused correction matrix of boundary bus B12.

The new coordinating equation (17) can guarantee accurate SE results. It can be seen that in the deductions of (17), approximations are only applied to the partial derivatives given by (16), which are the same as the FDSE algorithm. The measurement function $\boldsymbol{h}$ still uses the AC power flow model. Thus, (17) is essentially a combination of accurate coordinating equation (15) with FDSE algorithm. According to [22], the FDSE possesses good estimation quality. Therefore, the new coordinating equation is able to produce accurate SE results.

There are several merits of the new coordinating equation (17) as below.

- Regional correction matrices can be generated and shared before the peer-to-peer coordination. After obtaining these correction matrices from neighboring dispatch centers, a local coordinator can form fused correction matrices for all boundary buses, which can adjust boundary bus states according to (17) by itself.
- If topologies of regional grid 1 and 2 remain unchanged, $\boldsymbol{J}_{B12}^{1}$ and $\boldsymbol{J}_{B12}^{2}$ will also be invariant. Thus, they can be reused for the proposed FD2SE algorithms even when load levels of regional power grids change.
- During the peer-to-peer coordination, only $\Delta\boldsymbol{F}_{B12}^{1}$ and $\Delta\boldsymbol{F}_{B12}^{2}$ are exchanged by neighboring dispatch centers. As they have the same dimension as the boundary bus state $\boldsymbol{x}_{B12}$, communication costs of the proposed FD2SE tend to be very tiny.
- Equation (17) is obtained by integrating FDSE with the original coordinating equation (15). The partial derivative matrices in (15) are approximated to fixed matrices, using the same methods adopted by FDSE. Thus the new coordinating equation can ensure the accuracy of the estimation results.
- It is impossible to infer any internal bus states and topology information according to the above data exchanging. Thus, the information privacy of regional power grids will be guaranteed.

V. ASYNCHRONOUS CONVERGENCE DETECTING DURING FULLY DISTRIBUTED SE

A. FD2SE ALGORITHM EXECUTED BY LOCAL COORDINATORS

Taking the local coordinator of the region 2 as an example, we present the FD2SE algorithm as the following steps.

Step 1 (Initialization): A vector of initial values is given to states of boundary buses. Then, local topology analyses are carried out to obtain regional correction matrices, which are shared by neighboring regions in a peer-to-peer manner. Then, fused correction matrices, as well as their inverses, can also be generated easily for all boundary buses. For region 2, it forms $\boldsymbol{J}_{B12}^{-1}$ and $\boldsymbol{J}_{B23}^{-1}$ during this initialization stage.

Step 2: Local SE solution. The local SE of regional grid 2 is carried out to obtain the regional residual allocation factors $\Delta\boldsymbol{F}_{B12}^{2}$ and $\Delta\boldsymbol{F}_{B23}^{2}$. A local reference bus is chosen in the regional grid 2.

Step 3: Data Exchange. Peer-to-peer data exchanges are carried out by neighboring local dispatch centers, in order to share regional residual allocation factors of boundary buses. Then, values of the right side items in (17) can be evaluated for each boundary by a local coordinator individually. For region 2, it just needs to calculate $\Delta\boldsymbol{F}_{B12} \triangleq \Delta\boldsymbol{F}_{B12}^{1} + \Delta\boldsymbol{F}_{B12}^{2}$ and $\Delta\boldsymbol{F}_{B23} \triangleq \Delta\boldsymbol{F}_{B23}^{2} + \Delta\boldsymbol{F}_{B23}^{3}$.

Step 4: Convergence judging. Any boundary that reaches the balance of the residual reallocations will stop further adjustment of its bus states. If residual reallocations are balanced for all boundaries, then the global convergence is achieved and the iterations can be stopped. Otherwise, go to Step 5. For the boundaries of regional grid 2, such a balance requires $\|\Delta\boldsymbol{F}_{B12}\| < \varepsilon$ for B12 and $\|\Delta\boldsymbol{F}_{B23}\| < \varepsilon$ for B23. Here $\|\cdot\|$ is the infinite norm of a vector. ε is the convergence tolerance of the FD2SE algorithm, which is a small positive value.

Step 5: Update boundary state vectors. Adjustments of boundary state vectors are obtained by $\Delta\boldsymbol{x}_{B12} = \boldsymbol{J}_{B12}^{-1}\Delta\boldsymbol{F}_{B12}$ and $\Delta\boldsymbol{x}_{B23} = \boldsymbol{J}_{B23}^{-1}\Delta\boldsymbol{F}_{B23}$. Update the boundary state vectors and then go back to Step 2.

It should be noted that there is a local reference bus in each regional grid, while the coordination of different local reference buses is critical in solving the multi-region SE problem. In [7], the phase angle rotation approach is proposed and employed to match the phase angles of local reference buses to the global reference bus. Here in the proposed FD2SE algorithm, the same approach can be adopted. Moreover, in real dispatch centers where PMU measurements are available, another commonly used approach is to directly adopt PMU measurements of local reference buses. The feasibility of such an approach can be supported by two major aspects as follows. First, in real-time operations, regional grids are connected physically and synchronously, so local reference buses are naturally matched. Second, the PMU devices installed on local reference buses are of high qualities, so the produced measurements are very accurate. Thus both approaches can solve the inconsistency among local reference buses, while the second one tends to be easier to be applied in real scenarios.

B. JUDGING GLOBAL CONVERGENCE LOCALLY AND ASYNCHRONOUSLY

It is mentioned in Step 4 that the global convergence is achieved only when residual reallocations on all boundaries are balanced. However, in the fully distributed coordination, a local dispatch center acquires only the status of its own boundary buses, while there is no centralized coordinator being aware of states of all boundary buses. Thus, it is reasonable to have each local coordinator to judge the global convergence locally and asynchronously. That is, when residual reallocations are balanced on its own boundary buses, a local coordinator will stop updating corresponding boundary bus states.

It has been mentioned before that according to Section III, the distributed SE based on KKT condition decomposition can converge to the same optimal solution as the one obtained by the centralized SE. Moreover, the FD2SE adopts exactly the same method to simplify correction matrices as FDSE. Thus, its convergence rate almost equals to the centralized SE using the FDSE algorithm. In the following context, we will further elaborate that asynchronously stopping updating boundary states will not influence the global convergence of FD2SE.

Suppose that residual reallocations on boundary bus B12 are balanced after $t-1$ times of coordination. According to (14) and (16), at the t coordination, the adjustment of internal bus states of regional grid 2 should be

$$\Delta \boldsymbol{x}_2^t = -(\boldsymbol{B}_2^T \boldsymbol{G}_2 \boldsymbol{B}_2)^{-1} \boldsymbol{B}_2^T \boldsymbol{G}_2 \boldsymbol{B}_{B12}^2 \Delta \boldsymbol{x}_{B12}^t. \tag{18}$$

Then, a scale factor can be defined as below,

$$\alpha \triangleq \|(\boldsymbol{B}_2^T \boldsymbol{G}_2 \boldsymbol{B}_2)^{-1} \boldsymbol{B}_2^T \boldsymbol{G}_2 \boldsymbol{B}_{B12}^2\|_\infty \tag{19}$$

where $\|\cdot\|_\infty$ is the l_∞ matrix norm. According to [23], we can further obtain (20) as below,

$$\begin{aligned}\|\Delta \boldsymbol{x}_2^t\| &= \|(\boldsymbol{B}_2^T \boldsymbol{G}_2 \boldsymbol{B}_2)^{-1} \boldsymbol{B}_2^T \boldsymbol{G}_2 \boldsymbol{B}_{B12}^2 \Delta \boldsymbol{x}_{B12}^t\| \\ &\leq \|(\boldsymbol{B}_2^T \boldsymbol{G}_2 \boldsymbol{B}_2)^{-1} \boldsymbol{B}_2^T \boldsymbol{G}_2 \boldsymbol{B}_{B12}^2\|_\infty \cdot \|\Delta \boldsymbol{x}_{B12}^t\| \\ &= \alpha \|\Delta \boldsymbol{x}_{B12}^t\| < \alpha\varepsilon, \end{aligned} \tag{20}$$

where ε is the convergence tolerance of iterative coordination. It should be noted that if the distributed SE is converging to a global result gradually, the adjustment of boundary states tends to decrease. Thus, as residual reallocations are balanced on boundary bus B12 at the $t-1$ coordination, we can have $\Delta \boldsymbol{x}_{B12}^t < \Delta \boldsymbol{x}_{B12}^{t-1} < \varepsilon$.

It can be seen that the scale factor α determines the feasibility of judging the global convergence locally and asynchronously. If $\alpha < 1$, $\|\Delta \boldsymbol{x}_2^t\|$ will be smaller than the tolerance. Then, the iterative solution of the local SE of the region 2 will not be conducted as variations of internal bus states are tiny. Consequently, the early stopping of adjusting states of boundary bus B12 has no influences on states of other boundary buses of region 2. Fortunately, when adopting the FD2SE algorithm, α is a constant value associated with the network topology, parameters, and the weighting matrix. Thus, we can check the $\alpha < 1$ during the initialization stage of the FD2SE algorithm.

As a summary, judging global convergence can be performed locally and asynchronously, due to following two reasons. First, it is no need to adjust states of boundary buses, on which residual reallocations are balanced. Second, stopping state adjustments on balanced boundary buses will not affect iteratively updating states of other boundary buses.

Obviously, all above derivations can be extended to coordinate state adjustments for multiple boundary buses. Readers can change the subscript of variables used from 12 to 13 or 23 symmetrically. Moreover, although the above derivations are carried out for boundary buses shared by two adjacent regions, there are no limitations on the number of regional grids owning the same boundary buses. Therefore, similar derivations can be conducted to boundary buses connecting to more than two regional grids.

VI. CASE STUDY

The FD2SE algorithm is tested on three systems, including the revised IEEE 39, IEEE 118 bus system [24], and a real power grid from the southwest part of China (XN power grid). The FD2SE algorithm, as well as the system models, are developed in Matlab 2014. Simulations are carried out using a personal computer with 2 Intel Core i5-3230M CPUs running at 2.60 GHz (8.00 GB). The TCP/IP protocol with Socket API is used for the communication among dispatch centers in the Local Area Network (LAN). It should be noted that normally, dispatch centers communicate only through private networks, which are physically disconnected from the Internet. So the security of related data exchange can be guaranteed. The IEEE systems are relatively small, on which tests are carried out to validate the accuracy and convergence of the proposed algorithm. Data exchange amounts required by different DSE methods are also compared to demonstrate the communication efficiency of the FD2SE algorithm. The test on the XN power grid is applied to verify the feasibility of the proposed algorithm on a large scale interconnected power system with varied operating conditions. All three test systems are decomposed into three interconnected regional grids, whose parameters are listed in Table 1.

It should be noted that this work has been implemented in the real dispatch system of the State Grid Corporation of China. The dispatch system is named D5000 Platform [25], which integrates data and models to the dispatch management applications. Referring to the D5000 Platform, similar system models and computation procedures are adopted in the case study. When designing the cases, some aspects should be mentioned as below.

- The proposed FD2SE is applied to interconnected power systems with existing topological structures of regional grids. So the partitioning method of the test system is not the scope of this paper. In real systems, regional grids are decided by the administrative areas, such as the provinces and states. In this work, the XN power grid is a real system comprising of three provincial grids. So division of this system is according to the provinces. As for IEEE systems, the division is referred to relevant works in [7], [26].
- The states of boundary buses are measured by dispatch centers of all adjacent grids. In practice, these boundary buses are usually important substations that should be monitored by each side of the adjacent regions. Therefore, in the test system models, we apply the node-tearing method to partition the regions at boundary buses.
- In transmission grids, there are usually no loads connecting to the boundary buses, so the boundary power injection should equal to zero. When partitioning the IEEE systems, there may exist boundary buses connecting to loads. Then, we introduce virtual buses with zero power injection as the boundary buses, while the original ones are regarded as the internal buses.
- A model checking process is carried out by each regional dispatch center before the SE process. It identifies the topology errors by ensuring that both two ends of each line exist, and the line powers and bus voltages are within certain ranges.

Furthermore, the default convergence tolerance ε is set to 10^{-4} for tests on IEEE systems, while 10^{-3} is used for tests on the XN power grid. When the flat start is adopted for initializing states of boundary buses, the voltage amplitudes and phase angles are initialized as 1.0 p.u. and 0 rad, respectively.

TABLE 1. Configurations of the test systems.

Region	Num. of buses	Num. of meas.	Boundary buses	Scale factor (α)		
				B12	B23	B13
Revised IEEE 39 bus system						
1	15	124	9,17	0.8092	-	0.9710
2	13	112	9,14	0.1713	0.9166	-
3	14	112	14,17	-	0.3518	0.7845
IEEE 118 bus system						
1	35	356	15,19,23,30	0.9821	-	0.9493
2	42	456	15,19,30,69, 81	0.6952	0.9902	-
3	47	484	23,69,81	-	0.7273	0.8570
XN power grid						
1	1039	10224	347	0.9980	-	-
2	1041	10240	347,2947	0.7436	0.9608	-
3	1039	10224	2947	-	0.9981	-

At the initialization stage, scale factors are evaluated for each regional grid, which are also listed in Table 1. It can be seen that all these scale factors are smaller than 1, which guarantees the feasibility of judging global convergence locally and asynchronously.

A. TEST RESULTS OF IEEE 39 BUS SYSTEM

In Table 1, parameters of the revised IEEE 39 bus system are presented. The revised IEEE 39 bus system is derived from the original one by removing the branch from bus 3 to bus 4. It should be noted that the total number of buses is 42, which is greater than 39. This is because the boundary buses are shared by both regions. Measurements used in this case include bus voltage amplitudes and phase angles, bus injected powers, and line powers. Measurement noises in this test system are modelled as independent Gaussian with zero mean [27]. Two standard deviations are considered, which are 0.02 p.u. and 0.04 p.u., respectively. For each deviation, we generate randomly 5 groups of measurement noises obeying the normal distribution. The number of local coordination of FD2SE with these noises are listed in Table 2, which is different for each boundary. Take group 1 for example, residual allocations on B12 are balanced after 33 rounds of adjusting boundary bus states, while 2 more local iterations are carried out to tune boundary bus states on B23 and 3 more local iterations are performed for B13. For noises from group 1, we further compare the states estimated by FD2SE with the CSE. Absolute errors of voltage amplitudes and phase angles are shown in Fig. 3, which are within the acceptance of accuracy. We can clearly see that when judging global convergence asynchronously, the FD2SE can still produce accurate results.

The bad data identification (BDI) is also an important part of the SE. In this work, the proposed FD2SE enables the distributed BDI, where regional grids can carry out the BDI locally. Specifically, in each regional dispatch center, the largest normalized residual principle is adopted. As indicated by [7], for a certain measurement m, its normalized residual r_{Nm} is defined as,

$$r_{Nm} = |r_m|/\sqrt{\Omega_{mm}} \tag{21}$$

where $\Omega = G^{-1} - H \cdot (H^T \cdot G^{-1} \cdot H) \cdot H^T$. To validate the feasibility, in each region grid, we set one internal measurement and one boundary measurement as the bad data. The values of their r_m, r_{Nm} and Ω_{mm} are presented in Table 3, and the results prove that both CSE and the FD2SE can identify the bad data in internal and boundary measurements.

TABLE 2. Convergence performance of FD2SE for IEEE 39 bus system.

Standard deviation (p.u.)	Group number	Number of local coordination		
		B12	B23	B13
0.02	1	33	35	36
	2	32	35	35
	3	32	34	35
	4	32	35	36
	5	31	34	34
0.04	6	32	34	35
	7	34	37	38
	8	33	35	36
	9	34	37	37
	10	33	36	36

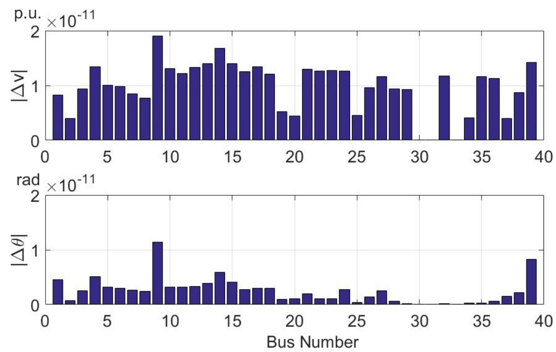

FIGURE 3. Absolute errors of states estimated by CSE and FD2SE for IEEE 39 bus system.

TABLE 3. Comparison between BDI in CSE and FD2SE.

Meas.	BDI in CSE			BDI in FD2SE		
	r_m (p.u.)	Ω_{mm}	r_{Nm}	r_m (p.u.)	Ω_{mm}	r_{Nm}
P2-1	0.6793	3.21×10^{-3}	11.99	0.6793	3.28×10^{-3}	11.85
P14-13	0.6007	3.93×10^{-3}	9.58	0.6007	4.03×10^{-3}	9.46
P15-14	0.6476	2.38×10^{-3}	13.28	0.6476	2.72×10^{-3}	12.42
Q5-4	0.6746	3.18×10^{-3}	11.97	0.6746	3.23×10^{-3}	11.87
Q22-21	0.6871	7.23×10^{-3}	8.08	0.6871	7.23×10^{-3}	8.08
Q9-39	0.6141	2.30×10^{-3}	12.82	0.6141	2.34×10^{-3}	12.70

B. TEST RESULTS OF IEEE 118 BUS SYSTEM

A partitioning scheme of IEEE 118 bus system is given in [24]. In this work, we adopt the same scheme, while including tie line 15-33, 19-34, 30-38 and 68-81 in region 2, as well as including tie line 23-24, 69-70, 69-75 and 69-77 in region 3. The measurements considered in this case are

TABLE 4. Performance of FD2SE for IEEE 118 bus system.

	Number of local coordination			Number of local SE iterations			Total exchanged floating-point data
	B12	B23	B13	Grid 1	Grid 2	Grid 3	
Group 1	3	3	2	10+9+7+5+3	11+9+7+4+3	12+10+7+4+2	260
Group 2	4	4	3	14+10+8+6+5+4	15+11+8+6+5+3	16+13+9+7+5+3	292
Group 3	5	4	3	14+10+8+6+5+4+3	14+10+8+6+4+3+1	15+12+10+7+5+2+1	304
Group 4	5	5	3	14+10+8+6+5+4+3	15+11+8+7+5+3+2	15+13+11+8+6+3+1	320
Group 5	3	4	3	15+10+9+7+5+1	15+11+9+7+5+3	16+12+9+7+5+2	280

TABLE 5. Comparison among FD2SE, SFHSE and D-RBSE for IEEE 118 bus system.

		FD2SE	SFHSE	D-RBSE
Iteration times	Local coordination / Outer iteration	3(B12); 3(B23); 2(B13)	1	25
	Local SE iterations	10+9+7+5+3(Grid 1) 11+9+7+4+3(Grid 2) 12+10+7+4+2(Grid 3)	12	
Exchanged floating-point data	Initialization	12+36(B12); 16+64(B23); 4+4(B13)	28	6/tie-line
	Iteration process	48(B12); 64(B23); 12(B13)	552	4/bus
Accuracy compared to CSE		10^{-7}	10^{-4}	10^{-4}

*In D-RBSE, only data exchange amount in each iteration is provided.

the same as the previous one. The parameter settings are referred to [7]. Standard deviation is set as 0.01 p.u. for power measurements and 0.001 p.u. for voltage measurements. The convergence tolerance is set as 0.001 for local SEs and 0.01 for FD2SE. Boundary bus states are initialized as the mean values of measurements obtained from neighboring grids on both sides of the boundary. In local SEs, internal bus states always start with the newest values, which can be obtained from the converged local SEs in the previous step. The initial bus states are set as the measurements.

Table 4 gives the results of 5 repeated tests for IEEE 118 bus system. The numbers with underline are the times of local SEs iterations during initialization. We can see that as FD2SE approaches the converged point, the numbers of local SE iterations gradually decrease since local SEs always start with the newest bus states. The total amount of floating-point data exchanged is dependent on the number of local coordination at each boundary. To further show the data exchange amount in each step, and compare the FD2SE with other algorithms, we take group 1 as an example to give Table 5.

In Table 5, the convergence rate, data exchange amount and accuracy of three DSE algorithms are compared. The Sensitivity Function based Hierarchical State Estimation (SFHSE) [7] is a hierarchical DSE method using the classic Newton iteration, where a centralized coordinator is required. The Distributed Robust Bilinear State Estimation (D-RBSE) [9] is a fully distributed SE method developed based on the ADMM theory, which improves the convergence through a two-stage linearization of the SE problem.

In terms of convergence, the outer iteration refers to the coordination of boundary bus states in SFHSE, which is executed by the central coordinator. The SFHSE needs only 1 outer iteration and 12 local SE iterations. Since SFHSE implements the classic Newton method, where the correction matrix is not approximated, its convergence is better than the FD2SE. As for D-RBSE, the SE problem has been linearized. So it only requires 25 ADMM iterations to obtain the results. Actually, the number of local SE iterations has no significant influences on the efficiency when using high-performance computation servers. In comparison, the FD2SE shows good convergence rate without complex reformulations of the SE problem, which allows it to be easily applied in practical dispatch systems.

During peer-to-peer coordination of the FD2SE, there are 260 floating-point data communicated among neighboring power grids totally. Take B12 as an example, 48 floating-point data are exchanged during the initialization, including boundary bus measurements (12 floating-point data) and regional correction matrices (36 floating-point data). Then, during iterations, totally 48 floating-point data are exchanged, which means that for each boundary bus, only 2 floating-point data are sent in 1 local coordination. The total exchanged floating-point data is 580 for SFHSE. The total number of D-RBSE is not directly given. However, as reported in [9], 6 floating-point data are exchanged per tie-line during initialization (first linear stage), after which 4 floating-point data are exchanged per boundary bus in each iteration (second linear stage). Thus, FD2SE requires the minimum data exchange amount among the three algorithms.

It should also be mentioned that the FD2SE adopts fully distributed coordination, which not only reduces the data exchange amount, but also eliminates global communication overheads caused by centralized coordination. Thus, this algorithm tends to be efficient and robust when applied in the wide-area network with uncertain and large latencies.

Furthermore, we also give the absolute errors of states estimated by CSE and FD2SE. In Fig. 4 we can see that the FD2SE can produce results very close to those of CSE.

C. TEST RESULTS OF XN POWER GRID

The three regional grids in XN power grid are formed as a chain connection. Region 1 and region 3 are not directly

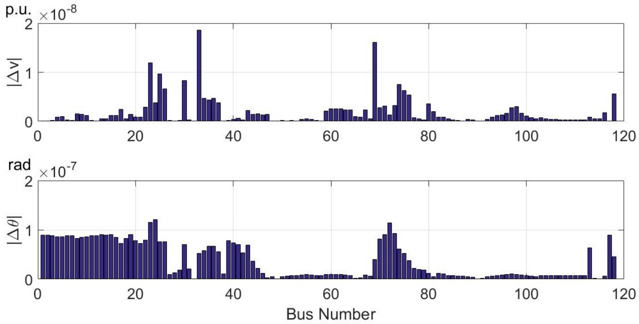

FIGURE 4. Absolute errors of states estimated by CSE and FD2SE for IEEE 118 bus system.

TABLE 6. Convergence performance respecting to system load levels.

Load levels (λ)	Number of iterations B12	B23	Exchanged floating-point data
1.0	8	9	76
1.1	9	9	80
1.2	10	10	88

connected, which means that there are only two groups of boundary buses such as B12 and B23. To verify the feasibility of the FD2SE algorithm on a real power system, tests are performed in scenarios with varied load levels as $\lambda = 1.0$ (base level), $\lambda = 1.1$ and $\lambda = 1.2$, and the results are presented in Table 6. Especially, we evaluate the extreme load level of the XN power grid by the continuation power flow, which is $\lambda = 1.28$. Thus, the proposed algorithm is tested in heavy load scenarios approaching the voltage collapse. The same measurements are used here as in previous cases.

From Table 6, we can know that the FD2SE is robust for solving the DSE of a large scale power system under varied load levels. The convergence rate of the proposed algorithm only slightly changes while the XN power grid is heavily loaded. Moreover, regional correction matrices remain constant when conducting the FD2SE algorithm, which even further improves the efficiency of online DSE applications.

Further, it should be noticed that as test systems scale up, the convergence rate of the proposed algorithm also increases. This is because that in large systems, the r/x ratio of lines is usually small. According to [22], the FDSE tends to fast converge for power systems with transmission lines having smaller r/x ratios. This feature also enhances the practicality of the FD2SE when applying to large interconnected power systems.

VII. CONCLUSION

In this paper, a fully distributed fast decoupled state estimation (FD2SE) algorithm is proposed to achieve peer-to-peer coordination of neighboring regional grids. To derive this algorithm, first the KKT condition of the global SE problem is obtained and decomposed according to territories of regional transmission grids. Then, the coordinating equation among local SEs is established. By employing the similar approximation used by the FDSE algorithm, coefficients of the coordinating equation are turned into constant values. In this way, data-exchange interfaces among regional grids are also simplified into fixed-matrix forms. Such interfaces enable the coordinating process to be fully distributed, which means that regional dispatch centers can detect the global convergence locally, and stop iterations asynchronously. Finally, by introducing a scale factor to evaluate different test systems, the feasibility of the fully distributed coordinating process is verified.

All of the above procedures comprise the integral FD2SE algorithm. Tests on IEEE systems further prove the feasibility and accuracy of the proposed algorithm. Compared with other DSE methods, the FD2SE shows better performance in convergence rate, and requires less amount of data exchange. Tests on the XN power grid further validate that the designed interface can be reused for multiple load levels. Finally, all of these tests show that the FD2SE achieves both the local detection of global convergence and asynchronous stopping of the computation. The relevant work in this paper has been applied in the practical dispatch centers of XN power grid.

In our future work, the topology identification can be further added to the FD2SE, which can provide a fully distributed solution to the topology error identification.

REFERENCES

[1] H. Ma, Y.-H. Yang, Y. Chen, and K. J. R. Liu, "Distributed state estimation in smart grid with communication constraints," in *Proc. Asia–Pacific Signal Inf. Process. Assoc. Annu. Summit Conf.*, Dec. 2012, pp. 1–4.

[2] Y. Ju, W. Wu, F. Ge, K. Ma, Y. Lin, and L. Ye, "Fast decoupled state estimation for distribution networks considering branch ampere measurements," *IEEE Trans. Smart Grid*, vol. 9, no. 6, pp. 6338–6347, Nov. 2018.

[3] J. Wang, Y. Chen, and C. Shen, "A method of distributed state estimation based on improved innovation graph," in *Proc. Joint Int. Conf. Power Syst. Technol. IEEE Power India Conf.*, Oct. 2008, pp. 1–5.

[4] Y. Guo, W. Wu, B. Zhang, and H. Sun, "An efficient state estimation algorithm considering zero injection constraints," *IEEE Trans. Power Syst.*, vol. 28, no. 3, pp. 2651–2659, Aug. 2013.

[5] M. Göl and A. Abur, "A fast decoupled state estimator for systems measured by PMUs," *IEEE Trans. Power Syst.*, vol. 30, no. 5, pp. 2766–2771, Sep. 2015.

[6] W. M. Lin and J. H. Teng, "Distribution fast decoupled state estimation by measurement pairing," *IEE Proc.-Generat., Transmiss. Distrib.*, vol. 143, no. 1, pp. 43–48, 1996.

[7] Y. Guo, L. Tong, W. Wu, H. Sun, and B. Zhang, "Hierarchical multi-area state estimation via sensitivity function exchanges," *IEEE Trans. Power Syst.*, vol. 32, no. 1, pp. 442–453, Jan. 2017.

[8] H. Zhu and G. B. Giannakis, "Power system nonlinear state estimation using distributed semidefinite programming," *IEEE J. Sel. Topics Signal Process.*, vol. 8, no. 6, pp. 1039–1050, Dec. 2014.

[9] W. Zheng, W. Wu, A. Gomez-Exposito, B. Zhang, and Y. Guo, "Distributed robust bilinear state estimation for power systems with nonlinear measurements," *IEEE Trans. Power Syst.*, vol. 32, no. 1, pp. 499–509, Jan. 2015.

[10] A. Minot and N. Li, "A fully distributed state estimation using matrix splitting methods," in *Proc. Amer. Control Conf. (ACC)*, Jul. 2015, pp. 2488–2493.

[11] A. Minot, Y. M. Lu, and N. Li, "A distributed Gauss-Newton method for power system state estimation," *IEEE Trans. Power Syst.*, vol. 31, no. 5, pp. 3804–3815, Sep. 2016.

[12] L. Xie, D.-H. Choi, and S. Kar, "Cooperative distributed state estimation: Local observability relaxed," in *Proc. IEEE Power Energy Soc. Gen. Meeting*, Jul. 2011, pp. 1–11.

[13] L. Xie, D. H. Choi, S. Kar, and H. V. Poor, "Fully distributed state estimation for wide-area monitoring systems," *IEEE Trans. Smart Grid*, vol. 3, no. 3, pp. 1154–1169, Sep. 2012.

[14] W. Zhang, W. Liu, C. Zang, and L. Liu, "Multiagent system-based integrated solution for topology identification and state estimation," *IEEE Trans. Ind. Informat.*, vol. 13, no. 2, pp. 714–724, Apr. 2017.

[15] D. Du, X. Li, W. Li, R. Chen, M. Fei, and L. Wu, "ADMM-based distributed state estimation of smart grid under data deception and denial of service attacks," *IEEE Trans. Syst., Man, Cybern., Syst.*, vol. 49, no. 8, pp. 1698–1711, Aug. 2019.

[16] L. Majzoobi, F. Lahouti, and V. Shah-Mansouri, "Analysis of distributed ADMM algorithm for consensus optimization in presence of error," *IEEE Trans. Signal Process.*, vol. 67, no. 7, pp. 1774–1784, Apr. 2019.

[17] G. N. Korres, "A distributed multiarea state estimation," *IEEE Trans. Power Syst.*, vol. 26, no. 1, pp. 73–84, Feb. 2011.

[18] F. C. Schweppe and J. Wildes, "Power system static-state estimation, Part I: Exact model," *IEEE Trans. Power App. Syst.*, vol. PAS-89, no. 1, pp. 120–125, Jan. 1970.

[19] L. Zhao and A. Abur, "Multi area state estimation using synchronized phasor measurements," *IEEE Trans. Power Syst.*, vol. 20, no. 2, pp. 611–617, May 2005.

[20] J.-W. Kang and D.-H. Choi, "Distributed multi-area WLS state estimation integrating measurements weight update," *IET Gener. Transmiss. Distrib.*, vol. 11, no. 10, pp. 2552–2561, 2017.

[21] S. Zhong and A. Abur, "Auto tuning of measurement weights in WLS state estimation," *IEEE Trans. Power Syst.*, vol. 19, no. 4, pp. 2006–2013, Nov. 2004.

[22] A. Garcia, A. Monticelli, and P. Abreu, "Fast decoupled state estimation and bad data processing," *IEEE Trans. Power App. Syst.*, vol. PAS-98, no. 5, pp. 1645–1652, Sep. 1979.

[23] C. D. Meyer, *Matrix Analysis and Applied Linear Algebra*, vol. 71. Philadelphia, PA, USA: SIAM, 2000.

[24] L. Min and A. Abur, "Total transfer capability computation for multi-area power systems," *IEEE Trans. Power Syst.*, vol. 21, no. 3, pp. 1141–1147, Aug. 2006.

[25] G. Yang, H. Chen, K. Zhang, Y. Wang, and F. Xu, "Modelling and design of wind power forecast error estimation system," in *Proc. IEEE Workshop Adv. Res. Technol. Ind. Appl. (WARTIA)*, Sep. 2014, pp. 1320–1323.

[26] Z. Ren, Y. Chen, S. Huang, and L. Zhang, "Searching severest VSM basing on CCPF among multiple dispatch centres," *IET Gener. Transm. Distrib.*, vol. 12, no. 6, pp. 1285–1293, Mar. 2018.

[27] A. Gomez-Exposito, C. Gomez-Quiles, and A. de la V. Jaen, "Bilinear power system state estimation," *IEEE Trans. Power Syst.*, vol. 27, no. 1, pp. 493–501, Feb. 2012.

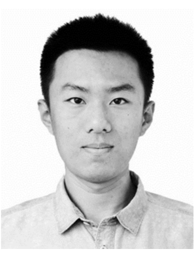

ZHENGWEI REN received the B.S. degree in electrical engineering from Xi'an Jiaotong University, Xi'an, China, in 2011. He is currently pursuing the Ph.D. degree in electrical engineering with Tsinghua University, Beijing, China. His research interests include distributed power flow, power system state estimation, and multi-energy system resilience.

YING CHEN (M'07) received the B.E. and Ph.D. degrees in electrical engineering from Tsinghua University, Beijing, China, in 2001 and 2006, respectively, where he is currently an Associate Professor with the Department of Electrical Engineering and Applied Electronic Technology. His research interests include parallel and distributed computing, electromagnetic transient simulation, cyber-physical system modeling, and cyber security of smart grids.

SHAOWEI HUANG (M'11) received the B.S. and Ph.D. degrees from the Department of Electrical Engineering, Tsinghua University, Beijing, China, in July 2006 and June 2011, respectively. From 2011 to 2013, he held a postdoctoral position at the Department of Electrical Engineering, Tsinghua University, where he is currently an Associate Professor. His research interests include power systems' modeling and simulation, power system parallel and distributed computing, complex systems and its application in power systems, and artificial intelligence.

MIGUEL HELENO received the M.Sc. degree in electrical engineering and computer science and the Ph.D. degree in sustainable energy systems within the MIT Portugal Program from the University of Porto. He is currently a Research Scientist with the Lawrence Berkeley National Laboratory, being the PI of projects in the field of optimal planning of microgrids and distribution systems. He has ten years of experience in power systems research both in Europe and USA, namely, in the topics of demand response, load flow, and OPF models.

YUE XIA received the B.S. and M.S. degrees in electrical engineering from China Agricultural University, Beijing, China, in 2009 and 2011, respectively, and the Ph.D. degree in electrical engineering from Technische Universität Berlin, Germany, in 2016. He currently holds a postdoctoral position with the Department of Electrical Engineering and Applied Electronic Technology, Tsinghua University. His research interests include power electronic systems, electrical machines, wind power, and modeling and simulation of power system transients.